THE ASTROPHYSICAL JOURNAL, 537:80–90, 2000 July 1

GAMMA-RAY AND MULTI–WAVE BAND EMISSION FROM GAMMA-RAY–LOUD BLAZARS

K. S. CHENG,[1] X. ZHANG,[1,2] AND L. ZHANG[1,3]

Received 1999 July 19; accepted 2000 February 7

ABSTRACT

Using multi–wave band data for 61 γ-ray–loud blazars (17 BL Lacertae objects and 44 flat-spectrum radio quasars [FSRQs]), we have studied the possible correlation between flux densities (F_R, F_K, F_O, F_X, and F_γ) in the radio, infrared, optical, X-ray, and γ-ray wave bands, in both the low and high states. For some blazars, it is hard to determine whether they are in a low or a high state because only one data point is available for each of them; initially, we exclude these blazars in our analysis. However, we include these blazars in later analysis by temporarily assuming them to be in a low state or a high state. Our main results are as follows. There are very strong correlations between F_X and F_O and between F_O and F_K in both low and high states. However, a strong correlation between F_X and F_K exists only in the low state. No definite correlation is found between γ-ray flux density and those of lower energy bands; however, there are hints of anticorrelation between F_γ and F_X as well as F_γ and F_O and a positive correlation between F_γ and F_R. From these results we suggest that (1) photons from infrared to X-rays are emitted by the same particles via synchrotron radiation and (2) if γ-rays are mainly produced by an inverse Compton scattering mechanism, it seems that the up-scattered soft photons are from external photons rather than synchrotron photons.

Subject headings: galaxies: active — gamma rays: observations — radiation mechanisms: nonthermal — quasars: general — X-rays: galaxies

1. INTRODUCTION

More than 60 γ-ray sources detected by EGRET around 1 GeV have been identified as blazars (Fichtel et al. 1994; von Montigny et al. 1995; Thompson et al. 1995; Nolan et al. 1996; Sreekumar et al. 1996; Lin et al. 1996; Dingus et al. 1996; Hartman et al. 1999). Furthermore, the Whipple Observatory has detected three BL Lac objects above 300 GeV: Mrk 421 (Punch et al. 1992), Mrk 501 (Quinn et al. 1996), and PKS 2344+514 (Catanese et al. 1998); the last one has not been detected yet by EGRET. Although the origin of the strong and variable high-energy emission is still not clear, the properties of the detected blazars strongly suggest that relativistic motion and beaming of the emitted radiation are required. Theoretically, a large γ-ray luminosity emitted in a compact volume is attenuated via photon-photon absorption, a mechanism that tends to reprocess γ-rays into softer (mainly X-ray) photons (Dondi & Ghisellini et al. 1995). For GeV or TeV energies, a high density of soft photons is required for photon-photon pair production. Many models have been proposed to explain the origin of the blazar γ-ray emission, including synchrotron self-Compton (e.g., Maraschi et al. 1992), inverse Compton scattering on photons produced by the accretion disk (Dermer, Schlickeiser, & Mastichiadis 1992; Zhang & Cheng 1997), scattered by ambient material, or reprocessed by the broad-line clouds (Sikora, Begelman, & Rees 1994; Blandford 1993; Blandford & Levinson 1995; Xie, Zhang, & Fan 1997), synchrotron emission by ultrarelativistic electrons and positrons (e.g., Ghisellini et al. 1993; Cheng, Yu, & Ding 1993), and electromagnetic cascade by collision of ultrarelativistic nucleons (e.g., Mannheim & Biermann 1992; Mannheim 1993; Cheng & Ding 1994). However, there is no consensus yet on the dominant emission process. These emission models imply various correlations in different wavelengths that can be used to distinguish among them observationally. Of course, simultaneous multiwavelength observations and the variability in various bands are more useful for establishing the correlation of γ-ray emission with emission across the electromagnetic spectrum from radio to X-ray. This is the key to understanding the origin of γ-ray emission. Dondi & Ghisellini (1995) have studied the correlation between γ-ray emission and the emission in the radio, optical, and X-rays in the form of luminosity for the entire sample of sources detected by EGRET. They found that the γ-ray luminosity is better correlated with the radio luminosity than with the optical or the X-ray luminosity. Xie et al. (1997) found that the γ-ray luminosity is better correlated with the infrared luminosity than with that from the optical or X-ray bands. However, in a flux-limited sample that covers a wide range of redshift, a correlation can appear in luminosity even though there is no intrinsic correlation in the sources because the luminosity is strongly correlated with redshift (Mücke et al. 1997). We use correlations between flux densities in different wave bands because they are less susceptible to such distortions.

In this paper, we collect 61 γ-ray–loud blazars and restudy in detail the correlation between the flux densities of different wave bands. Briefly, we make a statistical analysis of F_γ and F_X, F_γ and F_O, F_γ and F_K, F_γ and F_R, F_X and F_O, F_X and F_K, F_X and F_R, F_O and F_K, F_O and F_R, and F_K and F_R. It should be pointed out that in view of the large variations in the flux of all the bands considered, simultaneous observations should be used. Unfortunately, only a small number of EGRET sources have multi–wave band fluxes; thus, most of the multiband observations used here are not simultaneous. Lacking simultaneous multi–wave band data for the sources, we seek to define the minimum flux in differ-

[1] Department of Physics, University of Hong Kong, China.
[2] Beijing Astronomical Observatory, Chinese Academy of Science, Beijing, China.
[3] Department of Physics, Yunnan University, Kunming, China.

TABLE 1

BLAZAR SAMPLE

Source (1)	Name (2)	z (3)	Class Type (4)	F_K (mJy) (5)	Ref. (6)	F_X (μJy) (7)	Ref. (8)	F_γ (9)	Ref. (10)	F_R (Jy) (11)	Ref. (12)	F_O (mJy) (13)	Ref. (14)
0202+149......	4C 15.05	1.202	RQ	...	...	0.06	1	5.28 ± 2.64	2	3.68 ± 0.04	3	0.017	4
	...	...	HP	...	...	0.04	5	2.36 ± 0.56	2	1.56 ± 0.11	3	0.005	6
0208−512......	PKS	1.003	RQ	...	...	0.71 ± 0.03	1	13.41 ± 2.49	2	3.31 ± 0.12	7	0.85	8
	...	...	HP	...	...	0.181 ± 0.04	9	3.5 ± 1.1	2	...	...	0.364	10
0219+428......	3C 66A	0.444	BL	29.92 ± 0.59	11	1.25 ± 0.02	1	2.53 ± 0.58	2	2.55 ± 0.03	3	9.84 ± 0.98	12
	...	...	HP	6.79 ± 0.95	11	0.16	13	1.21 ± 0.39	2	0.52 ± 0.04	14	1.14 ± 0.06	12
0234+285......	CTD	1.213	RQ	...	...	0.19	15	3.41 ± 1.16	2	4.87 ± 0.06	3	0.186	7
	...	...	HP	...	...	0.09	1	1.09 ± 0.44	2	1.45 ± 0.04	7	0.10	4
0235+164......	OD	0.940	BL	199.53 ± 9.98	11	1.56 ± 0.31	16	6.51 ± 0.88	2	4.23 ± 0.02	3	7.06 ± 0.56	12
	...	...	HP	1.26 ± 0.04	11	0.17	13	1.16 ± 0.4	2	0.23 ± 0.05	3	0.64 ± 0.03	12
0336−019......	CTA 26	0.852	RQ	...	...	0.112	15	17.76 ± 3.66	2	2.29 ± 0.11	7	0.45	1
	...	...	NP	1.036	8	0.05	15	1.31 ± 0.76	2	1.18 ± 0.08	17	0.17	18
0420−014......	PKS	0.915	RQ	12.82 ± 0.51	19	0.52 ± 0.15	20	6.42 ± 3.42	2	6.99	17	1.00	8
	...	...	HP	1.16 ± 0.05	19	0.38	21	0.93 ± 0.47	2	2.03 ± 0.11	3	0.296	10
0440−003......	NRAO 190	0.844	RQ	...	...	...	...	8.59 ± 1.2	2	1.67 ± 0.08	7	0.145	10
	...	...	LP	...	...	<0.1	15	2.23 ± 0.41	2	1.18 ± 0.02	22	0.075	15
0446+112......	PKS	1.207	RQ	...	...	...	...	10.9 ± 1.94	2	1.89 ± 0.02	3	0.039	7
	...	...	NP	...	...	...	...	0.63 ± 0.33	2	0.50 ± 0.03	3	0.037	6
0454−234......	PKS	1.009	RQ	...	...	...	...	1.47 ± 0.42	2	2.15 ± 0.07	3	0.91	23
	...	...	HP	3.56 ± 0.01	24	0.055	18	0.81 ± 0.26	2	1.49 ± 0.08	3	0.04	23
0454−463......	PKS	0.858	RQ	...	...	...	...	2.28 ± 0.74	2	1.90 ± 0.09	7	0.527	8
	...	...	LP	...	...	0.16	1	0.55 ± 0.26	2	...	...	0.246	7
0458−020......	4C 2.19	2.286	RQ	...	...	0.1	1	6.82 ± 4.13	2	4.05 ± 0.06	3	0.17	7
	...	...	HP	...	...	0.04	21	0.95 ± 0.32	2	1.90 ± 0.05	3	0.057	25
0506−612......	PKS	1.093	RQ	...	...	...	...	2.88 ± 1.15	2	1.5 ± 0.08	7	0.7	26
	...	...	LP	...	...	0.28	1	0.64 ± 0.12	2	...	...	0.68	4
0521−365......	PKS	0.055	BL	38.73 ± 7.74	19	2.12	1	3.19 ± 0.72	2	8.87 ± 0.17	3	3.72 ± 0.13	27
	...	...	HP	17.50	19	0.68	21	1.95 ± 0.44	2	6.52 ± 0.16	3	1.0	28
0528+134......	OQ 147	2.07	RQ	...	...	2.32	29	35.1 ± 3.68	2	6.38 ± 0.10	3	0.308	1
	...	...	LP	...	...	0.12	5	3.24 ± 1.43	2	1.99 ± 0.04	3	0.06	10
0537−441......	PKS	0.896	BL	30.48 ± 1.82	11	0.79 ± 0.05	30	9.11 ± 1.46	2	5.30 ± 0.01	31	2.72	12
	...	...	HP	3.25 ± 0.10	11	0.12 ± 0.03	30	1.65 ± 0.45	2	2.52 ± 0.02	7	0.66	12
0716+714......	S5	0.3	BL	...	...	4.6	32	4.57 ± 1.11	2	1.17 ± 0.02	3	20.5	33
	...	...	HP	...	...	1.28	1	0.93 ± 0.47	2	0.31 ± 0.05	3	2.46	21
0735+178......	PKS	0.424	BL	49.20 ± 0.49	11	0.32	21	2.93 ± 0.99	2	4.82 ± 0.17	3	9.84 ± 0.69	12
	...	...	HP	5.50 ± 0.49	11	0.22 ± 0.03	16	1.58 ± 0.42	2	1.03 ± 0.03	3	0.95 ± 0.10	12
0804+499......	OJ 508	1.433	RQ	...	...	0.24 ± 0.01	34	1.51 ± 0.61	2	1.94 ± 0.13	3	0.39	7
	...	...	HP	...	...	0.17	1	0.83 ± 0.39	2	0.22 ± 0.04	3	0.37	6
0827+243......	OJ 248	2.050	RQ	...	...	0.34	1	11.1 ± 6.01	2	0.67	35	0.454 ± 0.13	36
	...	...	LP	...	...	0.097	15	1.56 ± 0.59	2	0.59 ± 0.01	22	0.21	37
0829+046......	OJ 049	0.18	BL	29.65 ± 0.18	11	1.07	38	3.35 ± 1.63	2	2.27 ± 0.2	3	3.09 ± 0.07	27
	...	...	HP	4.09 ± 0.29	11	0.19	21	1.68 ± 0.51	2	0.66 ± 0.18	3	0.62 ± 0.01	27
0836+710......	4C 71.07	2.172	RQ	...	...	2.20	1	3.34 ± 0.90	2	2.7 ± 0.07	3	1.47	39
	...	...	LP	...	...	1.11	1	0.86 ± 0.2	2	1.65 ± 0.09	3	0.91	10
0851+202......	OJ 287	0.306	BL	144.55 ± 4.34	11	2.16 ± 0.15	40	1.58 ± 0.69	2	5.01 ± 0.08	3	47.11 ± 9.81	12
	...	...	HP	5.35 ± 0.27	11	0.44	16	0.97 ± 0.44	2	0.99 ± 0.09	3	0.39 ± 0.02	12

TABLE 1—*Continued*

Source (1)	Name (2)	z (3)	Class Type (4)	F_K (mJy) (5)	Ref. (6)	F_X (μJy) (7)	Ref. (8)	F_γ (9)	Ref. (10)	F_R (Jy) (11)	Ref. (12)	F_O (mJy) (13)	Ref. (14)
0906+430......	3C 216	0.670	RQ	...	...	...	...	...	...	1.91 ± 0.05	3	0.383	18
	...	...	HP	1.0 ± 0.2	41	0.11	1	3.2 ± 0.9	42	1.27 ± 0.07	3	0.09	21
0917+449......	...	2.18	RQ	...	...	...	...	3.35 ± 1.3	2	2.34 ± 0.06	7	0.302	10
	...	...	...	...	...	0.47	1	1.14 ± 0.33	2	1 ± 0.02	22	0.065	1
0954+556......	4C 55	0.901	RQ	...	...	...	...	4.72 ± 1.55	2	2.29 ± 0.11	3	0.374	7
	...	...	HP	...	...	0.10	1	0.65 ± 0.25	2	1.71 ± 0.20	3	0.305	22
0954+658......	...	0.368	BL	...	...	0.5	32	1.80 ± 0.94	2	1.62 ± 0.03	3	1.84	8
	...	...	HP	...	...	0.16 ± 0.02	16	0.66 ± 0.17	2	0.18 ± 0.03	3	0.364	25
1101+384......	Mrk 421	0.031	BL	84.72 ± 6.77	11	272.8	43	2.71 ± 0.69	2	1.42 ± 0.11	3	39.18 ± 1.18	44
	...	...	HP	13.06 ± 0.65	11	7.9 ± 0.6	45	0.90 ± 0.36	2	0.43 ± 0.04	3	7.1	21
1127−145......	OM-146	1.187	RQ	...	...	0.34	1	6.18 ± 1.8	2	5.62 ± 0.17	7	1.06	8
	...	...	...	...	...	0.17	15	1.08 ± 0.59	2	2.95 ± 0.10	3	0.48	37
1156+295......	4C 29	0.729	RQ	75.86 ± 1.51	19	0.87 ± 0.12	45	16.3 ± 4.0	2	2.22 ± 0.04	3	17.91 ± 1.79	46
	...	...	HP	2.05 ± 0.1	19	0.44 ± 0.08	45	0.83 ± 0.2	2	0.88 ± 0.02	3	0.28 ± 0.06	46
1219+285......	ON 231	0.102	BL	13.43 ± 0.54	11	0.52	38	5.36 ± 1.41	2	2.39 ± 0.07	3	13.09 ± 0.13	12
	...	...	HP	1.39 ± 0.01	11	0.41	1	0.69 ± 0.26	2	0.54 ± 0.03	3	0.41 ± 0.01	12
1222+216......	4C 21	0.435	RQ	...	...	...	...	4.81 ± 1.53	2	2.23 ± 0.07	3	...	...
	...	...	...	...	...	0.41	1	0.69 ± 0.29	2	1.57 ± 0.10	3	0.39	1
1226+023......	3C 273	0.158	RQ	137.0 ± 2.0	47	21.0	20	4.83 ± 1.18	2	44.56 ± 0.38	3	49.33 ± 1.97	48
	...	...	LP	35.66 ± 0.16	49	11.15	38	0.85 ± 0.42	2	30.73 ± 0.89	3	20.95 ± 0.63	48
1229−021......	PKS	1.0448	RQ	...	...	0.08	1	1.55 ± 0.41	2	1.04 ± 0.03	7	0.699	6
	...	...	LP	...	...	0.06	15	0.49 ± 0.21	2	0.94 ± 0.03	3	0.699	6
1253−055......	3C 279	0.538	RQ	108.8 ± 3.3	19	1.34	1	26.7 ± 1.07	2	17.82 ± 0.12	3	90.59 ± 4.53	38
	...	...	HP	2.18 ± 0.32	19	0.63	20	0.76 ± 0.36	2	10.13 ± 0.29	3	0.29 ± 0.08	50
1313−333......	PKS	1.210	RQ	...	...	...	...	3.18 ± 1.9	2	1.47 ± 0.03	22	...	...
	...	...	NP	...	...	...	...	1.62 ± 0.53	2	1.21 ± 0.18	3	0.037	6
1331+170......	OP+151	2.0838	RQ	...	...	...	...	3.31 ± 1.93	2	...	...	...	...
	...	...	...	...	...	0.053	15	0.94 ± 0.27	2	0.70	17	0.76	51
1406−076......	PKS	1.494	RQ	...	...	...	...	12.84 ± 2.34	2	1.08 ± 0.04	7	...	...
	...	...	LP	...	...	...	...	1.04 ± 0.39	2	0.73 ± 0.04	3	0.17	7
1424−418......	...	1.522	RQ	...	...	...	...	5.53 ± 1.63	2	4.08 ± 0.14	7	1.05	8
	...	...	...	...	...	...	...	1.53 ± 0.86	2	2.18 ± 0.09	7	0.364	52
1510−089......	PKS	0.361	RQ	8.16 ± 2.53	19	0.87 ± 0.07	40	4.94 ± 1.83	2	4.33 ± 0.04	3	1.18	10
	...	...	HP	3.91 ± 0.35	19	0.44	21	1.26 ± 0.53	2	0.96 ± 0.14	3	0.62	21
1604+159......	4C 15	0.357	BL	...	...	...	...	4.2 ± 1.23	2	...	...	...	...
	...	...	HP	...	...	0.17	1	1.23 ± 0.47	2	0.5	21	0.13	21
1606+106......	4C 10	1.227	RQ	...	...	...	...	6.24 ± 1.3	2	1.98 ± 0.09	3	0.155	7
	...	...	LP	...	...	0.08	1	2.1 ± 0.92	2	1.07 ± 0.20	3	0.146	6
1611+343......	DA 406	1.404	RQ	0.98	8	0.24	1	6.89 ± 1.53	2	4.49 ± 0.03	3	0.55	8
	...	...	LP	0.68 ± 0.02	53	0.05	20	1.9 ± 0.4	2	2.07 ± 0.09	3	0.36	26
1622−253......	PKS 5	0.786	RQ	...	...	...	...	8.25 ± 3.5	2	2.34 ± 0.09	3	...	...
	...	...	LP	...	...	...	...	1.01 ± 0.40	2	1.53 ± 0.03	22	0.129	4
1622−297......	...	0.815	...	...	...	...	...	32.1 ± 3.35	2	3.97 ± 0.14	3	...	...
	...	...	...	...	...	0.08	1	1.24 ± 0.36	2	2.07 ± 0.09	3	0.367	1
1633+382......	4C 38	1.814	RQ	1.95 ± 0.07	53	0.42	1	10.7 ± 0.96	2	3.52 ± 0.03	3	0.401	8
	...	...	LP	1.61	8	0.08	20	3.18 ± 1.04	2	1.91 ± 0.02	3	0.25	10

TABLE 1—*Continued*

Source (1)	Name (2)	z (3)	Class Type (4)	F_K (mJy) (5)	Ref. (6)	F_X (μJy) (7)	Ref. (8)	F_γ (9)	Ref. (10)	F_R (Jy) (11)	Ref. (12)	F_O (mJy) (13)	Ref. (14)
1652+398......	Mrk 501	0.033	BL	54.96 ± 2.19	11	24.73	43	3.2 ± 1.3	54	1.96 ± 0.07	3	23.81 ± 3.34	44
	...	...	HP	15.14 ± 0.90	11	8.30 ± 0.13	16	1.8 ± 0.5	54	1.04 ± 0.13	3	8.11 ± 0.08	55
1730−130......	...	0.902	RQ	...	...	0.63	1	10.48 ± 3.47	2	9.01 ± 0.10	3	0.52	6
	...	...	...	...	...	0.22	15	1.81 ± 0.74	2	4.10 ± 0.05	3	0.14	9
1739+522......	4C 51	1.375	RQ	...	...	0.16	1	4.49 ± 2.69	2	3.36 ± 0.03	3	0.155	7
	...	...	HP	...	...	0.1	56	0.97 ± 0.47	2	0.58 ± 0.05	3	0.146	6
1741−038......	OT-68	1.054	RQ	...	...	0.75	9	4.87 ± 1.96	2	4.90 ± 0.06	3	0.735	8
	...	...	HP	...	...	0.61	1	1.76 ± 0.47	2	1.50 ± 0.09	3	0.132	6
1830−210......	...	1.000	...	...	...	...	...	9.93 ± 2.48	2	...	...	...	...
	...	...	...	...	...	0.43	9	1.78 ± 0.88	2	7.92	17	...	...
1933−400......	PKS	0.966	RQ	...	...	0.38	9	9.39 ± 3.14	2	1.48 ± 0.08	7	0.23	9
	...	...	NP	...	...	0.30	1	1.4 ± 0.34	2	0.66 ± 0.01	22	0.098	7
2005−489......	PKS	0.071	BL	35.98 ± 1.80	11	39.0 ± 1.06	45	...	...	1.23 ± 0.08	7	30	28
	...	...	HP	28.31 ± 0.85	11	2.02	45	1.8 ± 0.5	57	1.19 ± 0.04	58	7.0	32
2032+107......	PKS	0.601	BL	...	...	0.13	38	3.59 ± 1.50	2	1.08 ± 0.04	3	2.05	1
	...	...	HP	5.01	24	0.10	1	1.02 ± 0.38	2	0.26 ± 0.17	3	0.13	25
2052−474......	PKS	1.489	RQ	...	...	...	...	3.50 ± 2.09	2	...	...	0.296	7
	...	...	LP	...	...	0.28	9	1.13 ± 0.35	2	2.52 ± 0.1	7	0.084	6
2155−304......	PKS	0.116	BL	87.91 ± 2.64	19	46.0	43	3.04 ± 0.77	2	0.56 ± 0.07	3	44.9 ± 0.45	59
	...	...	HP	22.9 ± 1.14	19	3.07	40	0.79 ± 0.35	2	0.18 ± 0.09	3	8.11 ± 0.08	59
2200+420......	BL Lac	0.069	BL	178.66 ± 5.36	11	4.32	38	3.99 ± 1.16	2	9.98 ± 0.07	3	19.82 ± 1.19	12
	...	...	HP	20.70 ± 4.14	11	0.82	21	0.88 ± 0.38	2	1.69 ± 0.05	3	0.74 ± 0.06	12
2209+236......	PKS	...	RQ	...	...	...	...	4.57 ± 2.05	2	1.21 ± 0.16	60	...	...
	...	...	NP	...	...	...	...	1.23 ± 0.35	2	0.6 ± 0.13	3	0.098	61
2230+114......	CTA 102	1.037	RQ	...	...	0.75	15	5.16 ± 1.5	2	5.39 ± 0.14	3	0.70	8
	...	...	HP	...	...	0.29	1	1.21 ± 0.35	2	3.44 ± 0.08	3	0.364	10
2251+158......	3C 454	0.859	RQ	10.286	8	5.5 ± 1.65	62	11.61 ± 1.84	2	24. ± 0.72	7	2.28 ± 0.11	63
	...	...	HP	1.92 ± 0.19	19	0.61	21	2.46 ± 0.96	2	7.92 ± 0.14	3	0.66	64
2356+196......	PKS	1.066	RQ	...	...	...	...	2.63 ± 0.90	2	0.86 ± 0.08	3	0.246	61
	...	...	LP	...	...	0.28	1	0.83 ± 0.28	2	0.59 ± 0.10	3	0.23	6

REFERENCES.— (1) Comastri et al. 1997; (2) Hartman et al. 1999; (3) Data from the UMICH; (4) Impey & Tapia 1990; (5) Bregman et al. 1985; (6) Chiang et al. 1995; (7) Kuhr, Witzel, & Pauliny-Toth 1981; (8) Fossati et al. 1998; (9) Brinkman, Siebert, & Boller 1994; (10) Wall & Peacock 1985; (11) Fan & Lin 1999; (12) Fan & Lin 2000a; (13) Madejski & Schwartz 1983; (14) Weiler & Johnston 1980; (15) Wilkes et al. 1994; (16) Urry et al. 1996; (17) Mattox et al. 1997; (18) Maraschi et al. 1986; (19) Fan 1999; (20) Villata et al. 1997; (21) Ledden & O'Dell 1985; (22) Perley 1982; (23) Impey & Tapia 1988; (24) Allen, Ward, & Hyland 1982; (25) Wills et al. 1992; (26) Véron-Cetty & Véron 1991; (27) Falomo & Scarpa 1994; (28) Ghisellini et al. 1986; (29) Ghisellini et al. 1999; (30) Treves et al. 1993; (31) Komesaroff et al. 1984; (32) Wolter et al. 1994; (33) Bozyan, Hemenway, & Argue 1990; (34) Bloom et al. 1999; (35) Becker, White, & Edwards 1991; (36) Owen et al. 1978; (37) Maoz et al. 1993; (38) Worrall & Wilkes 1990; (39) Sambruna, Maraschi, & Urry 1996; (40) Sambruna et al. 1994b; (41) Landau et al. 1986; (42) Thompson et al. 1993; (43) Larner et al. 1996; (44) Sillanpää, Haarala, & Korhonen 1988; (45) Sambruna et al. 1994a; (46) Wills et al. 1983; (47) Courvoisier et al. 1988; (48) Türler et al. 1999; (49) Takalo et al. 1992; (50) O'Dell et al. 1978; (51) Wilkes et al. 1994; (52) Quiniento & Echave 1990; (53) Bloom et al. 1994; (54) Kataoka et al. 1999; (55) Xie et al. 1996; (56) Bloom & Marscher 1991; (57) Fichtel et al. 1994; (58) Wall et al. 1986; (59) Fan & Lin 2000b; (60) Gregory & Condon 1991; (61) Dondi & Ghisellini 1995; (62) Makino 1989; (63) Angione 1971.

ent bands for those objects in which flux variability has been observed. For the outburst phase, we use the maximum observed flux in each band. From the observations (Webb et al. 1988; Xie et al. 1992, 1996), we see that the timescale of the quiescent phase is much longer than that of the outburst phase. In the wide range of theoretical models, the outburst is likely to be produced by more complex physical processes. Therefore, the quiescent state is simpler for understanding emission mechanisms. We chose the lowest fluxes, irrespective of the date of observations, in all wave bands for all of the γ-ray–loud blazars. Of course, it is difficult to determine the low γ-ray state with present EGRET data because of the low sensitivity and dynamic range of EGRET data; in many cases the low γ-ray state could be well below the lowest fluxes or upper limits because EGRET-detected blazars are heavily biased toward detection of objects in high states. For this reason we have also studied the correlation between F_γ and other bands' flux densities in the high state and that between the average γ-ray flux and the low state of the lower energy bands.

2. DATA DESCRIPTION

The relevant data for 61 γ-ray–loud blazars are listed in Table 1. The columns in this table are as follows.

1. IAU name.
2. Other name.
3. Redshift z.
4. Classification of the source (HP = highly polarized quasar; LP = low-polarization quasar; NP = no known polarization measurements; RQ = flat-spectrum radio quasar; BL = BL Lacertae object) according to the criteria of Ghisellini et al. (1993).
5. Flux density (F_K) in millijanskys in the K band: the first entry is for the high state, the second for the low state; the arrangement is the same for other bands.
6. References for near-IR data.
7. 1 keV X-ray flux density (F_X) in microjanskys.
8. References for X-ray data.
9. γ-ray flux above 100 MeV (F_γ) in units of 10^{-7} photons $\mathrm{cm}^{-2}\ \mathrm{s}^{-1}$.
10. References for γ-ray data.
11. 5 GHz radio flux density (F_R) in janskys.
12. References for radio data.
13. V band optical flux density (F_O) in millijanskys.
14. References for optical data.

In Table 1, all but two objects (0906+430 and 2005−489) have γ-ray fluxes in both the high and low states. For those two objects, we cannot be certain whether they are in a high state or a low state (the former is more likely). In the following analysis, we will consider three possible cases: (1) excluding the two objects, (2) assuming them to be in a high state (more likely), and (3) assuming them to be in a low state. A similar process is adopted for the data of other wave bands. For the X-ray band, flux densities are available for 55 blazars, but only 40 have been detected in both high and low states. Twenty-one of 25 with near-IR (K-band) observations show observations in both the high and low states. In the optical band (V band), all 61 blazars have fluxes, but only 51 of them have fluxes in both high and low states. Finally, for the radio band, 54 of 61 objects have been observed in both high and low states.

3. CORRELATION ANALYSIS OF FLUX DENSITIES BETWEEN VARIOUS WAVE BANDS

We convert the γ-ray photon flux into flux density at a given energy E (GeV), as follows. First, let

$$\frac{dN}{dE} = N_0 E^{-\alpha_{\rm ph}} , \quad (1)$$

where N_0 is a normalization and $\alpha_{\rm ph}$ is the photon spectral index given in the third EGRET catalog (Hartman et al. 1999); integrating the above relation from 100 MeV to 10 GeV and setting it equal to the observed photon flux, we get N_0. Second, we determine the average energy of the photons, $\langle E \rangle$. Then the flux density at $\langle E \rangle$ GeV is obtained by multiplying relation (1) by $\langle E \rangle$; i.e., $F_{\langle E({\rm GeV})\rangle} = \langle E({\rm GeV})\rangle N_0 \langle E({\rm GeV})\rangle^{-\alpha_{\rm ph}}$.

All flux densities are k-corrected according to $F_\nu = F_\nu^{\rm ob}(1+z)^{\alpha-1}$, where α is the spectral index ($f_\nu \propto \nu^{-\alpha}$) and $\alpha_R = 0.0$, $\alpha_O = \alpha_{\rm IR} = 1.0$, and $\alpha_X = 1.47$ for BL Lacertae objects, and $\alpha_X = 0.87$ for other sources (Comastri et al. 1997). Finally, $\alpha_\gamma = \alpha_\gamma^{\rm ph} - 1$.

Linear regression is applied to the relevant data to analyze the correlation of flux densities between different wave bands in both high and low states. The analysis results are given in Table 2. The principal results are as follows.

1. There is a weak anticorrelation between F_γ and F_X in the low state for 39 objects with observations in both low and high states (see Fig. 1a and Table 2).
2. If we assume that the sources with only one measurement of γ-ray or X-ray emission in Table 1 are in their low states, then the number of the sample is 55. A weak correlation between F_γ and F_X is obtained (see Table 2).
3. There are also weak correlations between F_γ and F_O in both low and high states (see Fig. 1a and Table 2).
4. There is no clear correlation between F_γ and F_K; the correlation coefficient $r = -0.10$ in the low state for 20 sources (see Fig. 1c).
5. There is no correlation between F_γ and F_R in the high state (see Table 2), but a weak correlation can be found in the low state (see Fig. 1d and Table 2).
6. From Table 2 and Figure 2a, one can see that there is a strong correlation between F_X and F_O in both states for 39 sources. There is a strong correlation between F_X and F_K in the low state (see Fig. 2b) and a weak correlation in the high state for 22 sources (see Table 2). However, there is no correlation between F_X and F_R in either the low state (see Fig. 2c) or the high state (Table 2).
7. For 21 sources whose infrared fluxes in the two states have been detected, we find strong correlation between F_O and F_K in both states (see Fig. 2d and Table 2).
8. For F_O and F_R, there is no correlation for the low state (Fig. 3a), but a weak correlation is found for the high state (see Table 2). There is no correlation between F_K and F_R in either the low (Fig. 3b) or the high state (Table 2).
9. For radio-selected BL Lac objects, there is no correlation between the fluxes of different wave bands in either low or high states except for $F_O \sim F_K$ and $F_O \sim F_X$ in the low state (see Table 2).
10. We also considered the correlation between the average γ-ray data (Hartman et al. 1999) and the data of the lower energy bands in the low state. Results similar to those

TABLE 2

LINEAR REGRESSION ANALYSIS

x	y	N	A_0	A_1	r	P	Class Type	Note
$\log F_\gamma$	$\log F_X$ (high state)	39	−2.91	−0.15	−0.33	0.03	RQ+BL	...
		24	−2.68	0.12	0.23	0.26	RQ	...
		15	−3.13	−0.13	−0.40	0.13	BL	...
		55	−2.94	−0.12	−0.27	0.04	RQ+BL	Add 16 sources
$\log F_\gamma$	$\log F_X$ (low state)	39	−3.64	−0.18	−0.40	0.01	RQ+BL	...
		24	−3.53	−0.11	−0.24	0.25	RQ	...
		15	−3.71	−0.15	−0.34	0.21	BL	...
		55	−3.65	−0.17	−0.37	5.9×10^{-3}	RQ+BL	Add 14 sources
		55	−3.49	−0.10	−0.19	0.16	RQ+BL	Using Hartman's data
$\log F_\gamma$	$\log F_O$ (high state)	50	−2.9	−0.14	−0.34	0.015	RQ+BL	...
		35	−2.80	0.05	0.10	0.54	RQ	...
		15	−2.91	−0.27	−0.47	0.07	BL	...
		58	−2.91	−0.11	−0.30	0.02	RQ+BL	Add 8 sources
$\log F_\gamma$	$\log F_O$ (low state)	60	−3.62	−0.15	−0.34	0.016	RQ+BL	...
		43	−3.56	−0.11	−0.23	0.19	RQ	...
		15	−2.91	−0.27	−0.47	0.072	BL	...
		60	−3.62	−0.13	−0.32	0.012	RQ+BL	Add 10 sources
		60	−3.46	−0.06	−0.12	0.36	RQ+BL	Using Hartman's data
$\log F_\gamma$	$\log F_K$ (high state)	20	−2.69	−0.20	−0.38	0.09	RQ+BL	...
		23	−2.70	−0.19	−0.43	0.038	RQ+BL	Add 3 sources
$\log F_\gamma$	$\log F_K$ (low state)	20	−3.58	−0.06	−0.10	0.65	RQ+BL	...
		25	−3.56	−0.05	−0.09	0.65	RQ+BL	Add 5 sources
		25	−3.34	−0.13	−0.24	0.24	RQ+BL	Using Hartman's data
$\log F_\gamma$	$\log F_R$ (high state)	59	−2.92	0.09	0.11	0.4	RQ+BL	...
		43	−2.82	0.25	0.30	0.05	RQ	Excluding 3C273
		16	−3.20	0.06	0.09	0.74	BL	...
$\log F_\gamma$	$\log F_R$ (low state)	59	−3.49	0.23	0.32	0.01	RQ+BL	Excluding 3C273
		43	−3.50	−0.01	−0.02	0.89	RQ	...
		16	−3.59	0.28	0.48	0.056	BL	...
		60	−3.37	0.29	0.37	3.6×10^{-3}	RQ+BL	Using Hartman's data
$\log F_X$	$\log F_O$ (high state)	39	−0.24	0.71	0.77	1.05×10^{-9}	RQ+BL	...
		23	−0.28	0.53	0.74	5.7×10^{-5}	RQ	...
		16	−0.85	1.32	0.74	1.0×10^{-3}	BL	...
		54	−0.35	0.77	0.78	2.6×10^{-12}	RQ+BL	Add 15 sources
$\log F_X$	$\log F_O$ (low state)	39	−0.25	0.79	0.84	1.15×10^{-11}	RO+BL	...
		23	−0.44	0.53	0.58	1.79×10^{-3}	RQ	Excluding 3C273
		16	−0.26	0.95	0.88	6.25×10^{-7}	BL	...
		54	−0.31	0.71	0.77	1.1×10^{-11}	RQ+BL	Add 15 sources
$\log F_X$	$\log F_K$ (high state)	21	−0.67	0.70	0.52	0.01	RQ+BL	...
		8	−0.60	0.55	0.67	0.072	RQ	...
		13	−0.76	0.80	0.33	0.27	BL	...
$\log F_X$	$\log F_K$ (low state)	21	−0.91	0.99	0.76	5.6×10^{-5}	RQ+BL	...
		8	−0.95	1.42	0.90	2.12×10^{-3}	RQ	...
		13	−0.92	0.91	0.68	0.01	BL	...
		27	−1.04	1.05	0.75	1.34×10^{-5}	RQ+BL	Add 4 sources
$\log F_X$	$\log F_R$ (high state)	39	−0.13	0.33	0.15	0.37	RQ+BL	...
		22	−0.61	0.67	0.53	0.01	RQ	Excluding 3C273
		16	0.66	−0.50	−0.20	0.45	BL	...
		54	−0.62	0.18	0.13	0.35	RQ+BL	Add 16 sources[a]
$\log F_X$	$\log F_R$ (low state)	39	−0.54	0.17	0.12	0.45	RQ+BL	...
		23	−0.78	0.40	0.36	0.09	RQ	...
		16	−0.13	0.22	0.17	0.52	BL	...
		55	−0.62	0.18	0.13	0.35	RQ+BL	Add 16 sources
$\log F_O$	$\log F_K$ (high state)	21	−0.52	0.93	0.83	2.9×10^{-6}	RQ+BL	...
		8	−0.68	1.08	0.94	5.9×10^{-4}	RQ	...
		13	0.20	0.52	0.42	0.15	BL	...
		25	−0.45	0.09	0.88	5.5×10^{-9}	RQ+BL	Add 4 sources
$\log F_O$	$\log F_K$ (low state)	21	−0.62	0.93	0.81	1.0×10^{-5}	RQ+BL	...
		8	−0.69	1.24	0.90	2.3×10^{-3}	RQ	...
		13	−0.55	0.81	0.71	7.0×10^{-3}	BL	...
		25	−0.77	0.99	0.74	2.0×10^{-5}	RQ+BL	Add 4 sources
$\log F_O$	$\log F_R$ (high state)	47	−0.02	0.82	0.34	0.02	RQ+BL	Excluding 3C273
		32	−0.44	1.02	0.60	2.46×10^{-4}	RQ	...
		16	0.11	0.14	−0.07	0.80	BL	...
		59	−0.13	0.93	0.40	1.5×10^{-3}	RQ+BL	Add 12 sources[a]
$\log F_O$	$\log F_R$ (low state)	48	−0.38	0.34	0.24	0.10	RQ+BL	...

TABLE 2—*Continued*

x	y	N	A_0	A_1	r	P	Class Type	Note
		32	−0.62	0.64	0.50	3.2×10^{-3}	RQ	...
		16	0.11	0.14	0.13	0.64	BL	...
		59	−0.51	0.09	0.05	0.68	RQ+BL	Add 11 sources
log F_K	log F_R (high state)	21	1.38	0.31	0.22	0.34	RQ+BL	...
		8	0.59	0.87	0.59	0.12	RQ	...
		13	0.94	0.40	0.40	0.17	BL	...
		25	1.06	0.65	0.39	0.05	RQ+BL	Add 4 sources
log F_K	log F_R (low state)	21	0.68	0.21	0.22	0.33	RQ+BL	...
		8	0.23	0.53	0.70	0.05	RQ	...
		13	1.68	0.16	0.15	0.61	BL	...
		25	0.63	0.21	0.22	0.29	RQ+BL	Add 4 sources

NOTE—The linear regression is obtained by considering x to be the independent variable and assuming a relation $y = A_0 + A_1 x$; N is the number of points, r is the correlation coefficient, and p is the chance probability. Units are janskys for F_R, millijanskys for F_O and F_K, and microjanskys for F_X and F_γ. Add to the sources only one measured value of the flux of γ-ray or X-ray or optical or near-IR emission in Table 2. Using Hartman's data means that the γ-ray data are from the average data given by Hartman et al. 1999 for the four phases.

[a] Excluding 3C 273.

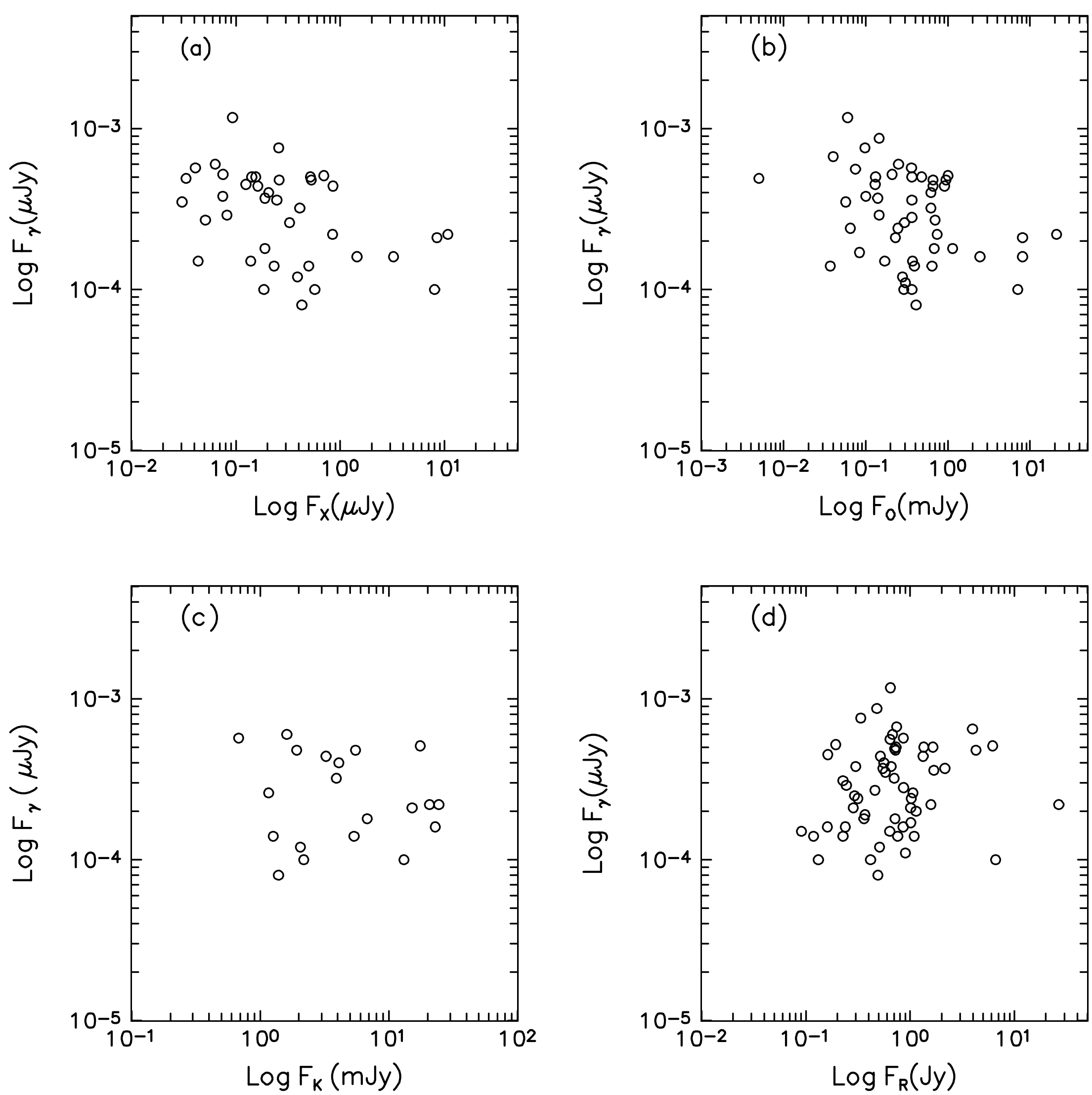

FIG. 1.—Correlations between γ-rays and four lower frequency bands

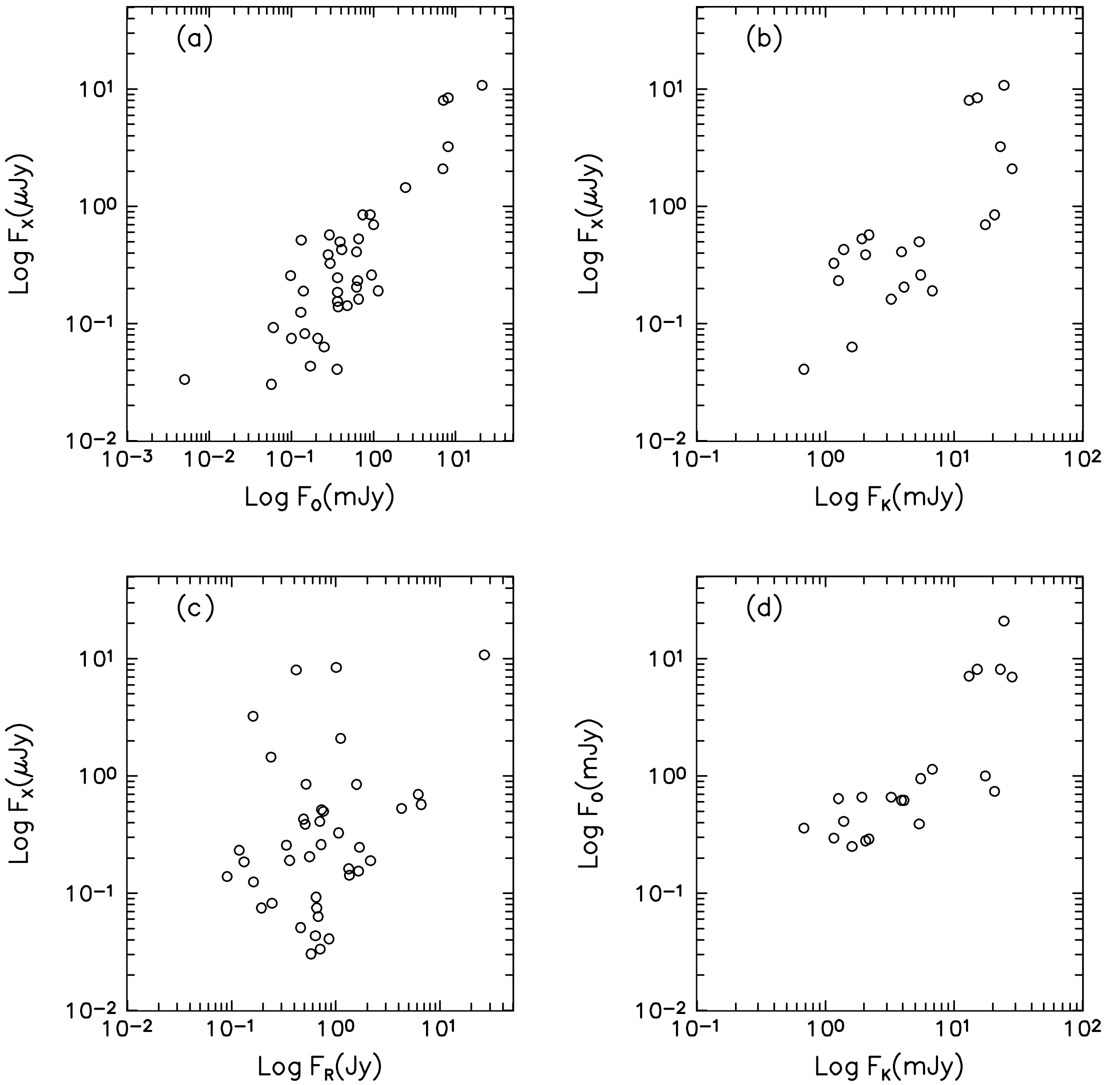

FIG. 2.—Correlations between X-rays and three lower frequency bands

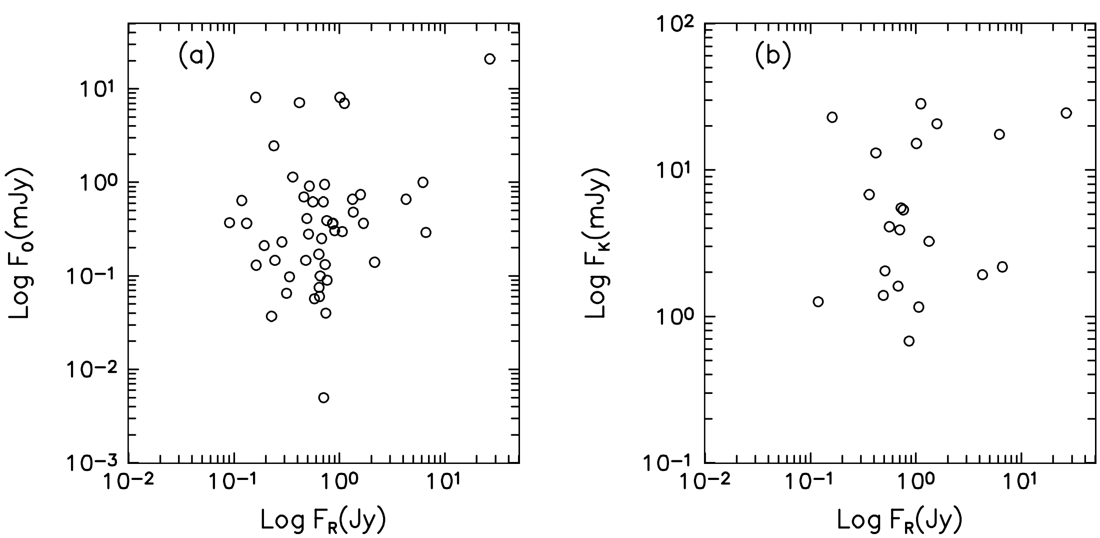

FIG. 3.—Correlations between optical and three lower frequency bands

corresponding to the above-mentioned ones have been found. They are

$$\log F_\gamma = (0.29 \pm 0.10) \log F_R - 3.37 \pm 0.04$$

with $r = 0.37$ and $p = 3.6 \times 10^{-3}$;

$$\log F_\gamma = -(0.13 \pm 0.11) \log F_K - 3.34 \pm 0.09$$

with $r = -0.24$ and $p = 24\%$;

$$\log F_\gamma = -(0.06 \pm 0.06) \log F_O - 3.46 \pm 0.05$$

with $r = -0.12$ and $p = 36.6\%$; and

$$\log F_\gamma = -(0.10 \pm 0.07) \log F_K - 3.49 \pm 0.06$$

with $r = -0.19$ and $p = 16\%$.

In summary, we find strong correlation between F_X and F_O and between F_O and F_K in both states and strong correlation between F_X and F_K only in the low state. There is only very weak anticorrelation between F_γ and F_X in the both low and high states. It should be reemphasized that the high state is not well defined. As seen in Table 1, for some blazars the differences between fluxes in high and low states are not significant. We have made the correlation analysis without any limit in the high state (see Table 2). Furthermore, we tried to use the condition that there is a factor of 5 difference of γ-ray fluxes between the high and low states to select samples, but under this condition, many objects have been excluded, and only a small sample can be obtained, for which there is no statistical significance.

The high states normally last for hours to days, so the lack of correlation among various wave bands may simply reflect the fact that the data of various wave bands were not taken simultaneously. On the other hand, low states (quiescent states) can last for many years, so it is much easier to catch blazars in the quiescent state for various wave bands, even though the observations are not simultaneous.

4. DISCUSSION

4.1. *Strong Constraints on Emission Regions of Various Wave Bands from γ-Ray–loud Blazars: RQs and BLs*

Table 3 qualitatively summarizes our results on γ-ray–loud blazars (detailed results are shown in Table 2). From Table 3 we may reach two conclusions: first, radio flux density is not correlated with those of other wave bands in either high or low states except for a weak correlation with γ-ray flux density. This strongly suggests that the emission region of radio photons in the jet is different from the emission regions of all other wave bands; second, infrared flux density is strongly correlated with optical and X-ray flux densities in the low state. This indicates that synchrotron radiation of high-energy electrons in the same emission region is likely to be responsible for the emission in the infrared, optical, and X-ray bands.

TABLE 3

SUMMARY OF CORRELATION ANALYSIS FOR γ-RAY BLAZARS

	F_R	F_K	F_O	F_X	F_γ
F_R	...	None	None	None	*p*
F_K	None	...	*P*	*P*	None
F_O	*p*	*P*	...	*P*	*n*
F_X	None	*p*	*P*	...	*n*
F_γ	None	*n*	*n*	*n*	...

NOTE—*P* = strong positive correlation, *p* = weak positive correlation, *N* = strong negative correlation, *n* = weak negative correlation, and none = no significant correlation.

4.2. *γ-Ray and X-Ray Emission from γ-Ray–loud Blazars*

The EGRET-detected active galactic nuclei (AGNs) share many common properties: flat radio spectrum, core dominance, and (for many) superluminal motion (von Montigny et al. 1995). The most striking common properties of these EGRET-detected AGNs are the large fraction of the bolometric power in the γ-ray bands and the rapid time variability, which ranges from as short as a few hours to several months in the high-energy γ-ray emission (see Mattox et al. 1997; Mukherjee et al. 1997; Wehrle et al. 1998; Cheng, Fan, & Zhang 1999; Fan, Xie, & Bacon 1999). Some of them are known to be BL Lac objects; many are recognized as optically violent variable/highly polarized quasars (OVV/HPQs). It is necessary to study this class of EGRET-detected AGNs together in order to understand the γ-ray emission mechanism. Using the sample of EGRET-detected sources listed in the first catalog of EGRET sources, Dondi & Ghisellini (1995) have found that all of them require relativistic bulk motion in order to be transparent to the γ-ray emission. Xie et al. (1997) found that the correlation between the γ-rays and the X-rays is not as close as that between the γ-ray and the infrared bands. In the present paper, we found that the γ-rays are anticorrelated with the X-rays; this anticorrelation for the flux density will dilute the correlation of luminosity found in the paper by Xie et al. (1997). A similar anticorrelation was also found in the spectral index plot (see Comastri et al. 1997). However, we should keep in mind that the low state used here is perhaps not the true low state of the source; also, the γ-rays may be more strongly beamed than the X-rays. Those effects would distort the correlation. Nevertheless, the correlation deserves to be investigated with more data when available. If this relation really does exist, then it will constrain the emission models.

4.3. *γ-Ray and Radio Emission from γ-Ray–loud Blazars*

The possible correlation between the radio and γ-ray luminosities of blazars has been studied by many authors (e.g., Padovani et al. 1993; Stecker et al. 1993; Dondi & Ghisellini 1995; Fan et al. 1998). A good correlation between radio and γ-ray luminosities for the γ-ray–loud blazars was found (e.g., Dondi & Ghisellini 1995). However, Mücke et al. (1997) have analyzed the correlation between the radio and γ-ray luminosities in detail and found no correlation. Recently Fan et al. (1998) revisited the correlation between radio and γ-ray fluxes using the observed maximum data in the γ-ray and radio bands. They found a very weak correlation between radio flux at 230 GHz and the γ-ray flux (the correlation coefficient is 0.347 for 44 objects) and almost no correlation between radio flux at 5 GHz and the γ-ray flux. From Table 2, our results show no correlation between radio flux at 5 GHz and γ-ray flux in either the high or the low state, which is consistent with the result of Fan et al. (1998). (If 3C 273 is excluded, there is a weak correlation between the γ-rays and the radio for the low state.) It is generally believed that both radio and γ-ray emission from the blazers are strongly beamed; both are produced in the jets of the blazars. However, the lack of correlation between radio and γ-ray emission or between radio and X-ray emission leads us to conclude that the radio, X-ray, and γ-ray emission regions are different.

4.4. *Other Wave Band Correlations*

For the correlation of optical and γ-ray emission, our results show that there is no correlation in the high state but a weak anticorrelation ($r = -0.34$ and $p = 1.5\%$) in the low state, implying that high γ-ray emission is correlated with low optical emission, consistent with the result of Dondi & Ghisellini (1995). The correlation between optical and infrared flux densities is expected since the two bands are so close in wavelength; they are both from the synchrotron process.

To take the correlations of the γ-rays and other lower bands into account, it is interesting to note that there is a weak anticorrelation between the γ-rays and the X-ray and optical bands, there is almost no correlation between the γ-rays and the infrared, but there is a positive weak correlation between the γ-rays and the radio band. If the synchrotron process is responsible for the emissions from the radio to the X-rays and inverse Compton scattering is responsible for the γ-rays, that inverse Compton scattering dominates the synchrotron process; an anticorrelation should be expected between the γ-rays and the optical to X-ray bands. As for the weak positive correlation between the γ-rays and the radio band, it implies that the same electron population is responsible for both the radio and the γ-ray bands. If this correlation is valid, it favors the external Compton (EC) scattering models. However, recent studies of broadband spectra of blazars indicate that (1) the synchrotron emission in X-ray–selected BL Lac objects extends well into X-rays, even to hard X-rays for Mrk 501 in a large TeV flare, and (2) the synchrotron emission in FSRQs seems to extend only to soft X-rays; the hard X-rays are inverse Compton emission, probably from the synchrotron self-Compton (SSC) process (Catanese et al. 1997; Sambruna 1997; Kubo et al. 1998; Mukherjee et al. 1999; Kataoka et al. 1999; Takahashi, Madejski, & Kubo 1999).

We are grateful to referee R. C. Hartman for his useful comments and suggestions and to J. H. Fan for his help with the data analysis. This research has made use of data from the University of Michigan Radio Astronomy Observatory, which is supported by funds from the University of Michigan. This work is partially supported by an Outstanding Researcher Award of the University of Hong Kong and a Croucher Foundation Senior Research Fellowship.

REFERENCES

Allen, D. A., Ward, M. J., & Hyland, A. R. 1982, MNRAS, 199, 969
Angione, R. J. 1971, AJ, 76, 25
Becker, R. L., White, R. L., & Edwards, A. L. 1991, ApJS, 75, 1
Blandford, R. D. 1993, in AIP Conf. Proc. 280, *Compton Gamma-Ray Observatory*, ed. M. Friedlander, N. Geherels, & D. J. Macomb (New York: AIP), 533
Blandford, R. D., & Levinson, A. 1995, ApJ, 441, 79
Bloom, S. D., & Marascher, A. P. 1991, ApJ, 366, 16
Bloom, S. D., Marascher, A. P., Gear, W. K., Aller, H., & Teräsranta, H. 1994, AJ, 108, 398
Bloom, S. D., et al. 1999, ApJS, 122, 1
Bozyan, E. P., Hemenway, P. D., & Argue, A. N. 1990, AJ, 99, 1421
Bregman, J. N., et al. 1985, ApJ, 291, 505
Brinkmann, W., Siebert, J., & Boller, T. 1994, A&A, 281, 355
Catanese, M., et al. 1998, ApJ, 501, 616
Catanese, M., et al. 1997, ApJ, 487, L143
Cheng, K. S., & Ding, K. Y. 1994, A&A, 288, 97
Cheng, K. S., Fan, J. H., & Zhang, L. 1999, A&A, 352, 32
Cheng, K. S., Yu, K. N., & Ding, K. Y. 1993, A&A, 275, 53
Chiang, J., et al. 1995, ApJ, 452, 156
Comastri, A., Fossati, G., Ghisellini, G., & Molendi, S. 1997, ApJ, 480, 534
Courvoisier, T. J.-L., et al. 1988, Nature, 335, 330
Dermer, C., Schlickeiser, R., & Mastichiadis, A. 1992, A&A, 256, L27
Dingus, B. L., et al. 1996, ApJ, 467, 589
Dondi, L., & Ghisellini, G. 1995, MNRAS, 273, 583
Falomo, R., & Scarpa, R. 1994, ApJS, 93, 125
Fan, J. H. 1999, preprint (astro-ph/9910269)
Fan, J. H., & Lin, R. G. 1999, ApJS, 121, 131
———. 2000a, ApJ, in press
———. 2000b, A&A, 355, 880
Fan, J. H., Xie, G. Z., & Bacon, R. 1999, A&AS, 136, 13
Fan, J. H., et al. 1998, A&A, 338, 27
Fichtel, C. E., et al. 1994, ApJS, 94, 551
Fossati, G., Maraschi, L., Celotti, A., Comastri, A., & Ghisellini, G. 1998, MNRAS, 299, 433
Ghisellini, G., Maraschi, L., Tanzi, E. G., & Treves, A. 1986, ApJ, 310, 317
Ghisellini, G., et al. 1993, ApJ, 407, 65
———. 1999, A&A, 348, 63
Gregory, P. C., & Condon, J. J. 1991, ApJS, 75, 1011
Hartman, R. C., et al. 1999, ApJS, 123, 79
Impey, C. D., & Tapia, S. 1988, ApJ, 333, 666
———. 1990, ApJ, 354, 124
Kataoka, J., et al. 1999, Astropart. Phys., 11, 149
Komesaroff, M. M., et al. 1984, MNRAS, 208, 409
Kubo, H., et al. 1998, ApJ, 504, 693
Kühr, H., Witzel, A., & Pauliny-Toth, I. I. 1981, A&AS, 45, 367
Landau, R., et al. 1986, ApJ, 308, 78
Larner, G., et al. 1996, A&A, 311, 384
Ledden, J. E., & O'Dell, S. L. 1985, ApJ, 298, 630
Lin, Y. C., et al. 1996, ApJS, 105, 331
Madejski, G. M., & Schwartz, D. A. 1983, ApJ, 275, 467
Makino, F. 1989, Proc. 23d ESLAB Symp. (ESA SP-295; Noordwijk: ESA), 803
Mannheim, K. 1993, A&A, 269, 67
Mannheim, K., & Biermann, P. L. 1992, A&A, 253, L21
Maoz, D., et al. 1993, ApJ, 409, 28
Maraschi, L., Ghisellini, G., & Celotti, A. 1992, ApJ, 397, L5
Maraschi, L., Ghisellini, G., Tanzi, E. G., & Treves, A. 1986, ApJ, 310, 325
Mattox, J. R., Schachter, J., Molnar, L., Hartman, R. C., & Patnaik, A. P. 1997, ApJ, 481, 95
Mattox, J. R., et al. 1997, ApJ, 476, 692
Mücke, A., et al. 1997, A&A, 320, 33
Mukherjee, R., et al. 1997, ApJ, 490, 116
———. 1999, ApJ, 527, 132
Nolan, P. L., et al. 1996, ApJ, 459, 100
O'Dell, S. L., Puschell, J. J., Stein, W. A., & Warner, J. W. 1978, ApJS, 38, 267
Owen, F. N., et al. 1978, AJ, 83, 685
Padovani, P., Ghisellini, G., Fabian, A. C., & Celloti, A. 1993, MNRAS, 260, L21
Perley, R. A. 1982, AJ, 87, 859
Punch, M., et al. 1992, Nature, 358, 477
Quiniento, Z. M., & Echave, M. M. 1990, A&AS, 83, 393
Quinn, J., et al. 1996, ApJ, 456, L83
Sambruna, R. M. 1997, ApJ, 487, 536
Sambruna, R. M., Barr, P., Giommi, P., Maraschi, L., Tagliaferri, G., & Treves, A. 1994a, ApJS, 95, 371
———. 1994b, ApJ, 434, 468
Sambruna, R. M., Maraschi, L., & Urry, C. M. 1996, ApJ, 463, 444
Sikora, M., Begelman, M. C., & Rees, M. J. 1994, ApJ, 421, 153
Sillanpää, A., Haarala, S., & Korhonen, T. 1988, A&AS, 72, 347
Sreekumar, P., et al. 1996, ApJ, 464, 628
Stecker, F. W., Salamon, M. H., & Malkan, M. A. 1993, ApJ, 410, L71
Takahashi, T., Madejski, G., & Kubo, H. 1999, Astropart. Phys., 11, 177
Takalo, L. O., et al. 1992, AJ, 104, 40
Thompson, D. J., et al. 1993, ApJ, 415, L13
———. 1995, ApJS, 101, 259
Treves, A., et al. 1993, ApJ, 406, 447
Türler, M., et al. 1999, A&AS, 134, 89
Urry, C. M., Sambruna, R. M., Worrall, D. M., Kollgaard, R. I., Feigelson, E. D., Perlman, E. C., & Stocke, J. T. 1996, ApJ, 463, 424
Véron-Cetty, M.-P., & Véron, P. 1991, A Catalog of Quasars and Active Nuclei (5th ed.; Garching: ESO)
Villata, M., et al. 1997, A&AS, 121, 119
von Montigny, C., et al. 1995, ApJ, 440, 525
Wall, J. V., Danziger, J. J., Pettini, M., Warwick, R. S., & Wamsteker, W. 1986, MNRAS, 219, P23
Wall, J. V., & Peacock, J. A. 1985, MNRAS, 216, 173
Webb, J. R., Smith, A. G., Leacock, R. J., Fitzgibbons, G. L., Gombola, P. P., & Shepherd, D. W. 1988, AJ, 95, 374

Wehrle, A. E., et al. 1998, ApJ, 497, 178
Weiler, K. W., & Johnston, K. J. 1980, MNRAS, 190, 269
Wilkes, B. J., Tananbaum, H., Worrall, D. M., Avni, Y., Oey, M. S., & Flanagan, J. 1994, ApJS, 92, 53
Wills, B. J., Wills, D., Breger, M., Antonucci, R. R. J., & Barvainis, R. 1992, ApJ, 398, 454
Wills, B. J., et al. 1983, ApJ, 274, 62
Wolter, A., Caccianiga, A., Della Ceca, R., & Maccacaro, T. 1994, ApJ, 433, 29
Worrall, D. M., & Wilkes, B. J. 1990, ApJ, 360, 396
Xie, G. Z., Zhang, Y. H., & Fan, J. H. 1997, ApJ, 477, 114
Xie, G. Z., et al. 1992, ApJS, 80, 683
———. 1996, AJ, 111, 1065
Zhang, L., & Cheng, K. S. 1997, ApJ, 488, 94